Ultrasensitive detection of pathological prion protein aggregates by dual-color scanning for intensely fluorescent targets

J. Bieschke*†, A. Giese*‡, W. Schulz-Schaeffer‡, I. Zerr§, S. Poser§, M. Eigen†, and H. Kretzschmar‡¶‖

†Max-Planck-Institute for Biophysical Chemistry, Am Fassberg, 37077 Göttingen, Germany; and Departments of ‡Neuropathology and §Neurology, University of Göttingen, Robert-Koch-Strasse 40, 37075 Göttingen, Germany

Contributed by M. Eigen, March 3, 2000

A definite diagnosis of prion diseases such as Creutzfeldt–Jakob disease (CJD) relies on the detection of pathological prion protein (PrP^{Sc}). However, no test for PrP^{Sc} in cerebrospinal fluid (CSF) has been available thus far. Based on a setup for confocal dual-color fluorescence correlation spectroscopy, a technique suitable for single molecule detection, we developed a highly sensitive detection method for PrP^{Sc}. Pathological prion protein aggregates were labeled by specific antibody probes tagged with fluorescent dyes, resulting in intensely fluorescent targets, which were measured by dual-color fluorescence intensity distribution analysis in a confocal scanning setup. In a diagnostic model system, PrP^{Sc} aggregates were detected down to a concentration of 2 pM PrP^{Sc}, corresponding to an aggregate concentration of approximately 2 fM, which was more than one order of magnitude more sensitive than Western blot analysis. A PrP^{Sc}-specific signal could also be detected in a number of CSF samples from patients with CJD but not in control samples, providing the basis for a rapid and specific test for CJD and other prion diseases. Furthermore, this method could be adapted to the sensitive detection of other disease-associated amyloid aggregates such as in Alzheimer's disease.

Creutzfeldt–Jakob syndrome | fluorescence spectrometry | diagnosis | cerebrospinal fluid | Alzheimer's disease

Prion diseases comprise a group of fatal transmissible neurodegenerative diseases. They are caused by an unusual transmissible agent that has been termed prion (1) and may occur as acquired, idiopathic, or hereditary diseases (2–4). Prion diseases include Creutzfeldt–Jakob disease (CJD) in humans as well as bovine spongiform encephalopathy and scrapie in animals. These diseases are characterized by the cerebral deposition of an aggregated pathological isoform of the prion protein termed PrP^{Sc}. PrP^{Sc} is found consistently in infectious preparations and is believed to be the essential component of the prion (4–6). PrP^{Sc} is thought to replicate by converting the normal cellular isoform of the prion protein (PrP^{C}) into the PrP^{Sc} state by a posttranslational process involving conformational changes (4, 7–9).

PrP^{C} is a copper-binding (10) cell surface glycoprotein normally found in neurons (11) and in other cell types (12, 13). PrP^{Sc} can be distinguished from PrP^{C} by its high content in β-sheet structure (7, 14), its partial resistance to protease digestion (6, 15), and its tendency to form large aggregates (16).

Detection of PrP^{Sc} by immunohistochemistry, Western blotting, or ELISA is used currently to reach a definite diagnosis of prion disease (17). However, these methods lack sufficient sensitivity to detect PrP^{Sc} in body fluids such as cerebrospinal fluid (CSF), although transmission studies indicate the presence of some infectivity in the CSF (18). Using an approach based on fluorescence correlation spectroscopy (FCS; refs. 19–21), we developed a highly sensitive method for detection of pathological PrP^{Sc} aggregates.

FCS in its current confocal form (22) has found widespread application as an analytical tool (23, 24). Recently, dual-color cross-correlation FCS (25, 26) has provided a method for the study of DNA hybridization, enzyme kinetics (27), and aggregation kinetics (28). It has been developed further for high-throughput screening in homogeneous assays (29, 30). Conventionally, FCS is used to study the dynamics of small monomeric proteins and polynucleotides at nanomolar to picomolar concentrations (24). Fluctuations caused by the diffusion of single fluorescently labeled molecules through an open volume element can be used to calculate the lateral diffusion coefficient and thus the size of the molecule (22). The volume element is defined by the beam of an excitation laser focused through a high aperture microscope objective and confocally imaged on a single photon-counting detector. The need for a sizable number of molecules to pass the focus limits the applicability of correlation analysis when measuring very rare targets.

By substituting part of the monomeric PrP with fluorescently labeled probe molecules, seed aggregates of pathogenic PrP^{Sc} (target) can become highly fluorescently labeled (28, 31). As the target molecule is rare, its signal has to be separated from that of unbound probe molecules, which are in excess up to a factor of 10^6. When passing the confocal detection volume, the target molecules emit a fluorescent burst up to 50 times stronger than the signal of free fluorescent probe molecules. Thus, target and probe can be separated by their relative fluorescent intensity. Application of this principle to the detection of disease-related amyloid aggregates of Aβ peptide in the CSF of patients with Alzheimer's disease has been reported recently (32).

Based on this principle, we developed an ultrasensitive quantitative detection method. By using a two-color scanning setup, pathological aggregates of PrP^{Sc} could be detected at femtomolar concentrations, which was sufficient to detect pathological aggregates of PrP^{Sc} in the CSF in cases of CJD.

Materials and Methods

rPrP (90–231) Labeling. Recombinant hamster PrP (90–231) prepared according to the method of Mehlhorn *et al.* (33), which was a kind gift from the group of D. Riesner (Heinrich-Heine-University, Düsseldorf, Germany) and of S. Prusiner (University of California, San Francisco), was labeled with an Oregon Green-labeling kit (Molecular Probes). Excess dye was removed by two gel-filtration steps with Sephacryl S-300 microspin col-

Abbreviations: CJD, Creutzfeldt–Jakob disease; CSF, cerebrospinal fluid; FCS, fluorescence correlation spectroscopy; SIFT, scanning for intensely fluorescent targets.

*J.B. and A.G. contributed equally to this work.

¶To whom reprint requests should be addressed. E-mail: Haus.Kretzschmar@inp.med.uni-muenchen.de.

‖Present address: Department of Neuropathology, University of Munich, Marchioninistrasse 17, 81377 München, Germany.

The publication costs of this article were defrayed in part by page charge payment. This article must therefore be hereby marked "*advertisement*" in accordance with 18 U.S.C. §1734 solely to indicate this fact.

umns (Amersham Pharmacia). Labeling efficiency was found to be 4%, assuming one fluorophore per protein molecule.

Antibody Purification and Labeling. Prion-protein-specific mAb 3F4 (34) was obtained from the group of H. Diringer and M. Beekes (Robert-Koch-Institute, Berlin). mAb 12F10 (ref. 35; Institut für Bioanalytik, Heiligenstadt, Germany) was purified from serum-free cell culture supernatant by means of a commercial protein G affinity purification kit (Amersham Pharmacia). Antibodies against IL-8 and Aβ (1–40) peptide were obtained from Sigma. For fluorescent labeling, 10 μg of antibody at 1 mg/ml in PBS was labeled with amino-reactive dyes (Alexa488-*O*-succinimidylester, Molecular Probes; Cy5-*O*-succinimidylester, Amersham Pharmacia). Excess dye was removed by gel filtration on a microspin column with Sephadex G 75 preequilibrated with PBS + 0.1% NP-40 (Sigma).

Prion Rods. Prion rods prepared from scrapie-infected hamster brain (31) were a gift from the group of D. Riesner. PrP^{Sc} concentration was determined to be 10 μg/ml in Western blotting by comparison with scrapie hamster brain.

Aβ (1–42) peptide (Sigma) was preaggregated at a concentration of 1 μM for 2 h in buffer containing 100 mM NaCl and 20 mM potassium acetate (pH 5). Prion rod and Aβ aggregate targets were diluted in pooled CSF of control patients or in buffer as indicated to a final volume of 20 μl. Labeled probes were added to a final concentration of 6 nM (antibodies) or 10 nM (rPrP). The sample was then filled contamination-free into a glass capillary of 0.2 $\times$ 2-mm diameter (VitroCom, Mountain Lake, NJ) and sealed onto a glass support.

CSF Samples. CSF of 24 patients with CJD (11 definite and 13 probable cases, according to established criteria for epidemiological surveillance; ref. 36) and of 13 control patients with the differential diagnosis of CJD that were classified as non-CJD was obtained; these patients were examined as part of the German CJD surveillance study. Samples were taken with informed consent in an ongoing study of diagnostic parameters for CJD approved by the local ethics committee.

Western Blotting. Prion rods were diluted in a pool of CSF from control patients without evidence of neurodegenerative disease. Scrapie-infected hamster brain (strain 263K) was homogenized in 9 volumes of lysis buffer (100 mM NaCl/10 mM EDTA/0.5% NP-40/0.5% sodium deoxycholate/10 mM Tris, pH 7.4) and treated with 100 μg/ml proteinase K at 37°C for 30 min. Digestion was terminated by addition of 5 mM PMSF and boiling in electrophoresis buffer [3% (wt/vol) SDS in 60 mM Tris (pH 6.8)]. Samples of 10 μl were run on an SDS/12.5% PAGE. After transfer to a nitrocellulose membrane (0.45 μm; Bio-Rad) immunodetection was performed with mAb 3F4 followed by goat anti-mouse IgG coupled to alkaline phosphatase (Dianova, Hamburg, Germany). Enzymatic activity was visualized with the CDP-Star chemiluminescent system (Tropix, Bedford, MA) and Hyperfilm ECL (Amersham Pharmacia) as described by the manufacturers.

FCS and Intensity Analysis Setup. Single-color experiments were carried out in a ConfoCor FCS setup (Zeiss). Dual-color experiments were performed in a dual-color FCS setup (28), originally developed by Schwille (25) in our laboratory and now built into a commercial prototype (Zeiss). The confocal detection volume of 0.44 fl was formed by the superimposed focal spots of an He-Ne laser (633 nm) and an Ar^+ laser (488 nm), exciting Cy5 and Alexa488 at a total power of 53 μW and 57 μW, respectively. Size and geometry of the focal volume were calculated from autocorrelation measurements with Rhodamine Green solution. The ConfoCor was equipped with a positioning table (Märzhäuser, Wetzlar, Germany) enabling scanning of the sample during measurement with a speed of 1 mm/s. The temperature for all measurements was 22°C, measurement time was 600 s. The fluorescent signal was split for correlation analysis and intensity analysis on a multichannel-scaler card with a channel time of 500 μs.

Results and Discussion

Quantification of Peak Fluorescent Signal. In pilot experiments, we tried to detect PrP^{Sc} in the CSF of patients with CJD by coaggregation of labeled PrP probes in a way similar to that described for the detection of Aβ aggregates in patients with Alzheimer's disease (32). By correlation analysis, the targeted PrP aggregates were shown to be both very large (>MDa) and very rare (data not shown). In fact, the number of detected targets and specificity of detection were not sufficient to allow a discrimination of CJD samples. Two challenges for fluorescent peak detection became apparent. First, the peak signal had to be quantified properly. Second, detection sensitivity and specificity had to be improved.

To detect quantitatively the signal of highly labeled target aggregates over a fluorescent background of unbound probe molecules, a simple cumulative on-line intensity analysis of the photocount signal was developed. Fluorescence photons were summed over time intervals of constant length. The number of channels in which a specific number of photons was counted was recorded in an intensity distribution histogram. The intensity distribution of a sample containing only free probe molecules is well defined and contains no signal above a certain threshold value (37). With intensely fluorescent targets present, an additional component of high fluorescence intensity is observed (Fig. 1), which was quantified by the number of channels above a threshold value.

Scanning for Intensely Fluorescent Targets (SIFT). Although intensity analysis provides an easy separation and quantification of target signal, it does not itself increase detection sensitivity. For large molecules at subpicomolar concentrations, slow diffusion becomes a limiting factor for detection (23). In contrast to conventional FCS, for intensity analysis, as well as cross-correlation analysis, the size information given by the diffusion time of the molecule is no longer needed, allowing the sample to be moved relative to the focus.

Samples were enclosed in a glass capillary, which was moved at a speed of 1 mm/s. This movement caused the average diffusion time τ_{DiH} of a PrP aggregate to decrease from 10–100 ms to a passage time τ_{flow} of about 0.5–1 ms (data not shown), thereby increasing the number of particles passing the volume about 100-fold when compared with static measurements. With τ_{Flow} being smaller than $1/10\ \tau_{Diff}$, diffusion processes can be discarded. The time an aggregate stays in focus is thus determined only by the mean displacement time of the focal volume and by the excitation profile. Therefore, the number of peak channels should be proportional to the number of target molecules, even for a small number of detected events.

The sensitivity of the method was evaluated with a diagnostic model system. To that purpose, pooled CSF of control patients was spiked with purified prion rods derived from Syrian hamster brain. With improved sensitivity, it became apparent that our rPrP probes already contained a significant intrinsic background of aggregated material, probably caused by self-aggregation, limiting the detection threshold for PrP^{Sc} to about 6 ng/ml (0.2 nM; Fig. 1 *A* and *B*). Using monomeric PrP as a probe molecule can induce further growth of the target aggregates employing the principle of seeded aggregation. However, because the target aggregates can be assumed to be large, incubation with fluorescently labeled PrP-specific antibodies also yields intensely fluorescent targets. Antibody probes showed

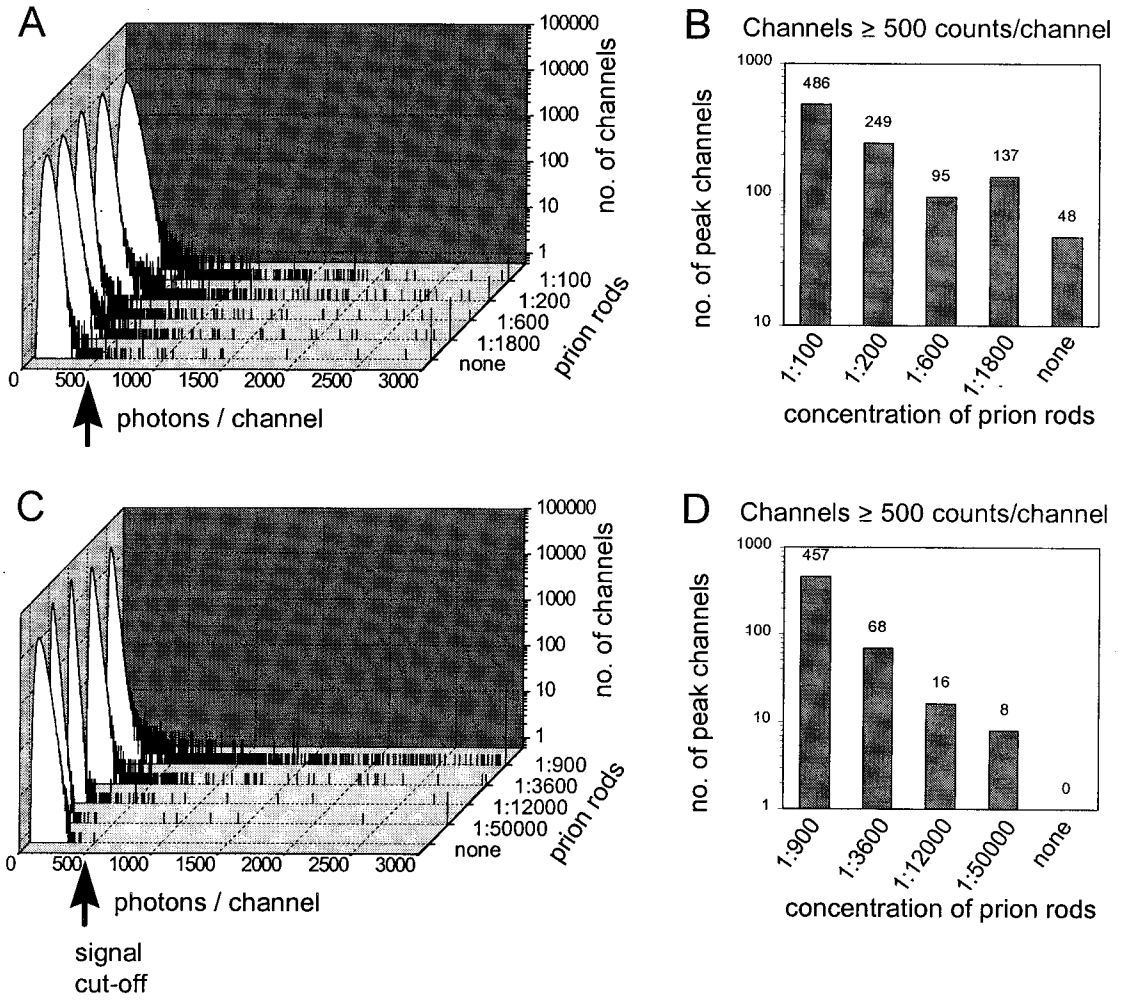

Fig. 1. Evaluation of different probe molecules. Hamster rPrP (90–231) labeled with Oregon Green (*A* and *B*) and mAb 3F4 labeled with Alexa488 (*C* and *D*) were added to pooled CSF of control patients that was spiked with prion rods derived from scrapie-infected hamster brain. Measurements were performed in a single-color SIFT setup with a channel width set at 500 μs and a scanning speed of 1 mm/s for a measurement time of 600 s. The high-intensity signal seen in the cumulative intensity distribution analysis (*A* and *C*) was quantified by counting the number of channels with ≥500 photons per channel (*B* and *D*). Whereas the rPrP probe contains a significant amount of intrinsic high-intensity signal, virtually no background signal is found in the antibody probe, which allows quantitative target detection to be made with very high sensitivity.

virtually no endogenous high-intensity signal, increasing detection sensitivity by almost two orders of magnitude (Fig. 1 *C* and *D*).

Dual-Color Intensity Distribution Analysis. To improve specificity, we further developed our assay by using two independent probes, tagged with different fluorescent labels (red and green). In the resulting two-color setup, two parameters can be used for the separation of target signal: (*i*) cross-correlation of the red and green signal and (*ii*) dual-color intensity distribution analysis to detect the target-derived, coincident high-intensity signal of both fluorescent labels. To that purpose, during a measurement time of 600 s, the number of red and green fluorescent photocounts was recorded for 1.2×10^6 consecutive channels of 500 μs. The fluorescence intensity distribution of channels was analyzed in a two-dimensional histogram, which can be displayed on-line during the measurement (Fig. 2). By this evaluation method, target molecules that simultaneously show a high fluorescent signal both in the red and the green detector channel are separated efficiently from the fluorescent signal of the free probe molecules. Moreover, they are separated from other particles—to which, unspecifically, only one of the fluorescent probes binds—and from aggregates of the probe molecule itself, thereby increasing specificity (Fig. 2*F*).

Evaluation of Detection Specificity and Sensitivity. The refined technique of dual-color SIFT was again evaluated by using prion rods as a diagnostic model system to assess the specificity of target recognition. Without the addition of a target to the control CSF sample, no specific binding occurred and virtually no high-intensity signal resulted (Fig. 2*C*). When aggregated Aβ (1–42) peptide was added as an unspecific amyloid target, no doubly labeled aggregates were detected either, although some unspecific binding of the 3F4 antibody was observed (Fig. 2*D*). To test for coincident binding of irrelevant probes, two probes directed against targets unrelated to CJD were added to CSF spiked with prion rods (Fig. 2*E*). Although antibody binding yielded highly labeled particles in each color, no coincident high fluorescent intensity signal was observed. Thus, we conclude that unspecific binding, which would produce the same signal as specific binding to PrP aggregates, is unlikely to occur under the chosen conditions.

To evaluate sensitivity, aliquots of diluted prion rod material were analyzed by Western blotting parallel to SIFT measure-

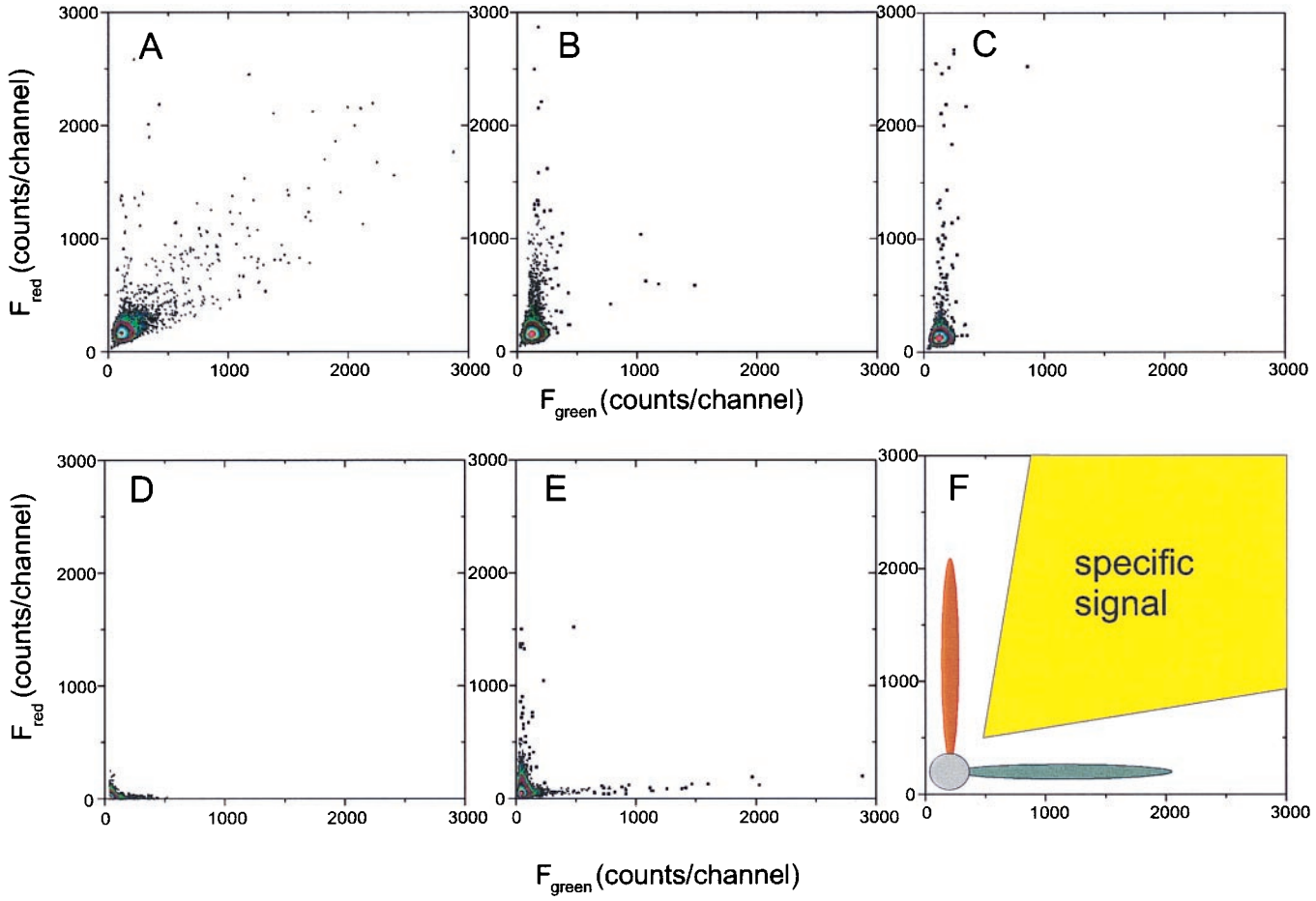

Fig. 2. Dual-color fluorescence intensity histogram. mAbs 3F4-Alexa488 and 12F10-Cy5 were added to pooled CSF of control patients that was spiked with prion rods derived from scrapie-infected hamster brain at various dilutions (*A*, 1:1,000; *B*, 1:100,000; *C*, no rods) or aggregates of Aβ (1–42) peptide at a concentration of 1 μM (*D*). (*E*) Unspecific antibody probes mAb(Aβ)-Alexa488 and mAb(IL-8)-Cy5 were added to prion rods diluted 1:1,000 in CSF. Samples were measured for 600 s with a channel time of 500 μs in an open volume element moving at 1 mm/s. Each dot represents a pair of fluorescent intensities. The number of channels is color-coded on a logarithmic scale. (*F*) Schematic representation of an intensity histogram. Low-intensity fluorescent signal of probe molecules (gray) is separated from unspecific aggregates incorporating only one type of label (red). Channels with a high-intensity signal in both colors above a linear cutoff (yellow) are summed for quantitative analysis (see Fig. 3). F_{red}, red fluorescence; F_{green}, green fluorescence.

ments (Fig. 3). The detection threshold of Western blotting for PrP^{Sc} was 1:10,000, corresponding to about 10 pg or 33 pM of monomeric PrP^{Sc} (38). By using dual-color SIFT, the concentration of prion rods was measured over more than four orders of magnitude with a detection threshold of a 200,000-fold dilution or 2 pM PrP^{Sc}. The fluorescence signal obtained during SIFT measurements was evaluated in parallel by cross-correlation analysis (27). However, at low target concentrations, dual-color SIFT proved to be more reliable than cross-correlation analysis. The mean error of the concentration determined by dual-color SIFT was 8% with a maximal error of 50% at detection threshold concentration. The mean peak signal of non-CJD control samples was 0.2 ± 0.4 channels; the maximum signal in control samples was 1 channel.

The physical detection limit for a single aggregate during a measurement time of 600 s (one particle in a volume of 1.2×10^6 times the focal volume of the confocal setup) corresponds to a concentration of 2 fM, assuming no distortion of the focal volume. Comparison of PrP concentration determined by Western blotting with aggregate concentration determined by SIFT yields an average of 10^3 PrP molecules per aggregate. Although subject to some experimental uncertainty of both concentration measurements, this number is clearly smaller than the amount of 10^5 to 10^6 PrP monomers that is contained in 1 infectious unit as determined by transmission studies (39).

Because little is known about the actual size of the infectious particle, no conclusion can be drawn as to whether the PrP aggregates are heterogeneous in infectivity or whether simply a large number of potentially infectious particles are needed to initiate the pathological process *in vivo*. Whichever is the case, it can be considered advantageous in terms of diagnostic sensitivity that the number of aggregates detected by our method seems to be much higher than the number of infectious units.

Detection of PrP^{Sc} Aggregates in the CSF of Patients with CJD. It was our primary aim to develop a highly sensitive diagnostic test for pathological PrP aggregates in CSF. After adding antibody probes, otherwise untreated CSF was analyzed for 10 min by SIFT. In 5 of 24 samples from patients with a probable or definite diagnosis of CJD, we could detect a specific high-intensity signal, whereas none of the samples derived from 13 non-CJD cases with neurodegenerative disease contained a positive signal, yielding a sensitivity of 21% and a specificity of 100% (Fig. 4). This value is the best for an agent-specific CSF test published thus far, because, even by using primates as highly susceptible experimental hosts, the transmission rate with CSF from patients

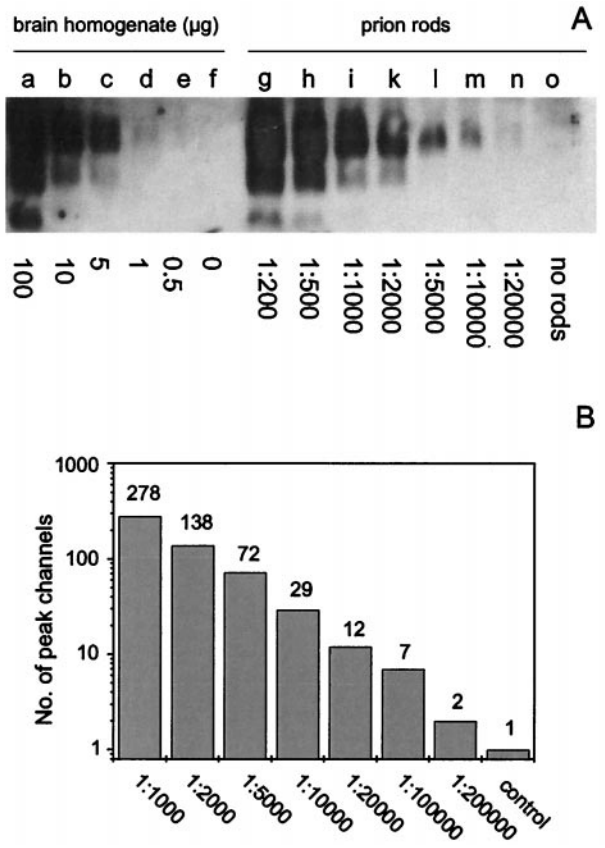

Fig. 3. Western blotting and dual-color SIFT measurement of prion rod dilution. (*A*) Brain homogenate of scrapie-infected hamster 263K (lanes a–f) and prion rod material (lanes g–o) in CSF was diluted as indicated. PrP^{Sc} was detected by Western blotting with 3F4 antibody after digestion with proteinase K (100 μg/ml) for 30 min at 37°C. (*B*) In parallel, aliquots of prion rod material were measured by dual-color SIFT, and the peak signal was quantified as in Fig. 2.

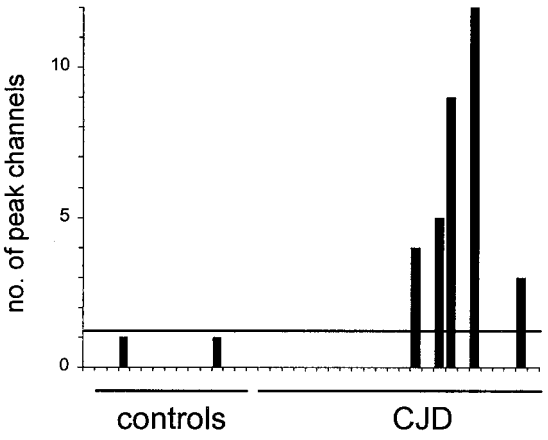

Fig. 4. Dual-color SIFT measurements in CSF samples. Measurements were performed for a measurement time of 600 s with a channel time of 500 μs with mAbs 3F4-Alexa488 and 12F10-Cy5 and analyzed as described in Fig. 3. By using a cutoff level of one high-intensity channel, a specific dual-color, high-intensity signal was found in 5 of 24 patients with probable or definite CJD, whereas none of the CSF samples from 13 non-CJD cases with neurodegenerative disease contained a positive signal.

with CJD was only 4 of 27 or 15% (18). However, a sensitivity of 21% remains somewhat unsatisfactory compared with established CSF parameters such as NSE and 14-3-3 protein, which in turn are not at all 100% specific, even when applied to a highly selected group of patients (40). It remains to be investigated whether pathological aggregates of PrP^{Sc} are present in measurable numbers in the CSF of all patients with CJD at all times. However, we believe that, with further improvement of our assay, the diagnostic sensitivity will also increase considerably. Preliminary experiments with purified prion rods suggest that by using a faster scanning speed, sensitivity can be increased by at least one order of magnitude. In addition, we suggest that further advances can be achieved by improved sample handling and by the combination of our detection system with established methods for purifying and concentrating PrP^{Sc}.

Conclusions

Single-molecule techniques have opened new windows on our understanding of biological, chemical, and physical processes. In this work, a twist to single-particle detection based on SIFT is presented and applied to the diagnosis of CJD. In comparison to published data on FCS-based amyloid detection (32), SIFT is based on four major technical advances. (*i*) A target-derived signal is quantified by analysis of fluorescence intensity distribution. (*ii*) Scanning increases detection sensitivity by two orders of magnitude. (*iii*) Use of antibody probes instead of monomeric building blocks with an inherent tendency for self-aggregation significantly improves the signal-to-noise ratio. (*iv*) Dual-color recording suppresses the signal from unspecifically bound probe molecules. It thus increases specificity and, in turn, increases detection sensitivity and allows further characterization of target aggregates by differential antibody binding. This approach could also open the way for direct prion strain typing, an interesting option not only for the differentiation of the bovine spongiform encephalopathy-derived new variant of CJD.

Current diagnostic tests based on surrogate markers have not attained the high degree of specificity that the SIFT-based direct detection of PrP^{Sc} should provide. The method has been shown to be 20 times more sensitive than Western blotting. In addition, direct detection of PrP^{Sc} in a homogeneous assay allows fast measurement of a large number of samples. More thorough scanning as well as improved sample handling and preparation promise to improve sensitivity significantly. Being by no means limited to the diagnosis of prion diseases, dual-color SIFT could provide a highly sensitive diagnostic test for amyloid aggregates in other disorders such as Alzheimer's disease and could be a valuable tool in drug development and therapy.

The PrP material was a gift from the groups of D. Riesner and of S. Prusiner; 3F4 antibody was obtained from the group of H. Diringer and M. Beekes. We thank P. Schwille for critical reading of the manuscript, C. Oberdiek for expert technical assistance, and Zeiss for technical cooperation. The work presented herein was supported by Grant 01 KI 9454/0 from the German Ministry for Education, Science, Research and Technology and by Grant 325-4471-02/15 from the German Ministry of Health and by the European Union.

1. Prusiner, S. B. (1982) *Science* **216,** 136–144.
2. Weissmann, C. (1996) *FEBS Lett.* **389,** 3–11.
3. Prusiner, S. B. (1993) *Arch. Neurol.* **50,** 1129–1153.
4. Prusiner, S. B. (1998) *Proc. Natl. Acad. Sci. USA* **95,** 13363–13383.
5. Bolton, D. C., McKinley, M. P. & Prusiner, S. B. (1982) *Science* **218,** 1309–1311.
6. Prusiner, S. B., Groth, D. F., Bolton, D. C., Kent, S. B. & Hood, L. E. (1984) *Cell* **38,** 127–134.
7. Pan, K.-M., Baldwin, M., Nguyen, J., Gasset, M., Serban, A., Groth, D., Mehlhorn, I., Huang, Z., Fletterick, R. J., Cohen, F. E., *et al*. (1993) *Proc. Natl. Acad. Sci. USA* **90,** 10962–10966.
8. Kocisko, D. A., Come, J. H., Priola, S. A., Chesebro, B., Raymond, G. J., Lansbury, P. T. & Caughey, B. (1994) *Nature (London)* **370,** 471–474.
9. Eigen, M. (1996) *Biophys. Chem.* **63,** A1–A18.
10. Brown, D. R., Quin, K., Herms, J. W., Madlung, A., Manson, J., Strome, R.,

Fraser, P. E., Kruck, T., von Bohlen, A., Schulz-Schaeffer, W., *et al*. (1997) *Nature (London)* **390,** 684–687.
11. Kretzschmar, H. A., Prusiner, S. B., Stowring, L. E. & DeArmond, S. J. (1986) *Am. J. Pathol.* **122,** 1–5.
12. Cashman, N. R., Loertscher, R., Nalbantoglu, J., Shaw, I., Kascsak, R. J., Bolton, D. C. & Bendheim, P. E. (1990) *Cell* **61,** 185–192.
13. Manson, J., West, J. D., Thomson, V., McBride, P., Kaufman, M. H. & Hope, J. (1992) *Development (Cambridge, U.K.)* **115,** 117–122.
14. Caughey, B. W., Dong, A., Bhat, K. S., Ernst, D., Hayes, S. F. & Caughey, W. S. (1991) *Biochemistry* **30,** 7672–7680.
15. Oesch, B., Westaway, D., Wälchli, M., McKinley, M. P., Kent, S. B. H., Aebersold, R., Barry, R. A., Tempst, P., Teplow, D. B., Hood, L. E., *et al*. (1985) *Cell* **40,** 735–746.
16. Prusiner, S. B., McKinley, M. P., Bowman, K. A., Bolton, D. C., Bendheim, P. E., Groth, D. F. & Glenner, G. G. (1983) *Cell* **35,** 349–358.
17. Kretzschmar, H. A., Ironside, J. W., DeArmond, S. J. & Tateishi, J. (1996) *Arch. Neurol.* **53,** 913–920.
18. Brown, P., Gibbs, C. J., Rodgers-Johnson, P., Asher, D. M., Sulima, M. P., Bacote, A., Goldfarb, L. G. & Gajdusek, D. C. (1994) *Ann. Neurol.* **35,** 513–529.
19. Magde, D., Elson, E. L. & Webb, W. W. (1972) *Phys. Rev. Lett*. **29,** 705–708.
20. Elson, E. L. & Magde, D. (1974) *Biopolymers* **13,** 1–27.
21. Ehrenberg, M. & Rigler, R. (1974) *J. Chem. Phys.* **4,** 390–401.
22. Rigler, R., Mets, Ü., Widengren, J. & Kask, P. (1993) *Eur. Biophys. J.* **22,** 169–175.
23. Eigen, M. & Rigler, R. (1994) *Proc. Natl. Acad. Sci. USA* **91,** 5740–5747.
24. Schwille, P., Bieschke, J. & Oehlenschläger, F. (1997) *Biophys. Chem.* **66,** 211–228.
25. Schwille, P. (1996) Dissertation (Technical University Braunschweig, Braunschweig, Germany).
26. Schwille, P., Meyer-Almes, F.-J. & Rigler, R. (1997) *Biophys. J.* **72,** 1878–1886.
27. Kettling, U., Koltermann, A., Schwille, P. & Eigen, M. (1999) *Proc. Natl. Acad. Sci. USA* **95,** 1416–1420.
28. Bieschke, J. & Schwille, P. (1997) in *Fluorescence Microscopy and Fluorescent Probes*, ed. Slavik, J. (Plenum, New York), Vol. 2, pp. 81–86.
29. Koltermann, K., Kettling, U., Bieschke, J., Winkler, T. & Eigen, M. (1998) *Proc. Natl. Acad. Sci. USA* **95,** 1421–1426.
30. Winkler, T., Kettling, U., Koltermann, A. & Eigen, M. (1999) *Proc. Natl. Acad. Sci. USA* **96,** 1375–1378.
31. Post, K., Pitschke, M., Schäfer, O., Wille, H., Appel, T. R., Kirsch, D., Mehlhorn, I., Serban, H., Prusiner, S. B. & Riesner, D. (1998) *Biol. Chem.* **379,** 1307–1317.
32. Pitschke, M., Prior, R., Haupt, M. & Riesner, D. (1998) *Nat. Med.* **4,** 832–834.
33. Mehlhorn, I., Groth, D., Stockel, J., Moffat, B., Reilly, D., Yansura, D., Willett, W. S., Baldwin, M., Fletterick, R., Cohen, F. E., *et al*. (1996) *Biochemistry* **35,** 5528–5537.
34. Kascsak, R. J., Rubenstein, R., Merz, P. A., Tonna-DeMasi, M., Fersko, R., Carp, R. I., Wisniewski, H. M. & Diringer, H. (1987) *J. Virol.* **61,** 3688–3693.
35. Krasemann, S., Groschup, M. H., Harmeyer, S., Hunsmann, G. & Bodemer, W. (1996) *Mol. Med.* **2,** 725–734.
36. World Health Organization (1998) *Wkly. Epidemiol. Rec.* **73**, 361–365.
37. Chen, Y., Muller, J. D., So, P. T. C. & YGratton, E. (1999) *Biophys. J.* **76**, A445–A445.
38. Meyer, R. K., McKinley, M. P., Bowman, K. A., Braunfeld, M. B., Barry, R. A. & Prusiner, S. B. (1986) *Proc. Natl. Acad. Sci. USA* **83**, 2310–2314.
39. Beekes, M., Baldauf, E. & Diringer, H. (1996) *J. Gen. Virol.* **77,** 1925–1934.
40. Zerr, I., Bodemer, M., Gefeller, O., Otto, M., Poser, S., Wiltfang, J., Windl, O., Kretzschmar, H. A. & Weber, T. (1998) *Ann. Neurol.* **43,** 32–40.